Optimization of spectrally flat and broadband single-pump fiber optic parametric amplifiers

Conference Paper *in* Optics Communications · November 2003

DOI: 10.1109/LEOS.2003.1251727 · Source: IEEE Xplore

4 authors, including:

Claudio Floridia
70 PUBLICATIONS 194 CITATIONS

L. de S. Menezes
Federal University of Pernambuco
93 PUBLICATIONS 1,451 CITATIONS

Anderson S L Gomes
Federal University of Pernambuco
443 PUBLICATIONS 5,688 CITATIONS

Available online at www.sciencedirect.com
SCIENCE DIRECT®
Optics Communications 223 (2003) 381–388
OPTICS COMMUNICATIONS
www.elsevier.com/locate/optcom

Optimization of spectrally flat and broadband single-pump fiber optic parametric amplifiers

Claudio Floridia, M.L. Sundheimer, L. de S. Menezes, A.S.L. Gomes *

Departamento de Física, Universidade Federal de Pernambuco, 50670-901 Recife, PE, Brazil

Received 26 January 2003; received in revised form 4 April 2003; accepted 30 May 2003

Abstract

Using well-known theory for fiber optical parametric amplifiers in the no-depletion approximation, a simple condition relating the second- and fourth-order dispersion parameters β_2 and β_4 is demonstrated which ensures ripple-free, broadband gain spectra using realistic fiber parameters. Inclusion of pump depletion gives rise to expressions which enable optimization of fiber length and the maximum achievable ripple-free gain.

PACS: 42.79.S; 42.81; 42.65.Y

Keywords: Optical communication systems; Fiber optics; Optical parametric amplifiers

1. Introduction

Fiber optical parametric amplifiers (FOPAs) have been intensively studied in recent years due to their potential use for amplification and wavelength conversion in multi-terabit/s dense wavelength division multiplexing (DWDM) transmission systems [1–13]. FOPAs have the advantage of being able to operate in any of the telecom bands (S–C–L) depending upon pump wavelength and the fiber zero-dispersion wavelength, which, in principle, can be appropriately tailored.

In order to be a practical amplifier in a DWDM system, the FOPA should exhibit high gain, large bandwidth and should be spectrally flat, among other requirements. Researchers have recently demonstrated a broadband FOPA with 49 dB gain using a multi-segment fiber design [2], and a very broadband (200 nm, considering both the signal and idler bands) Raman-assisted FOPA [6]. Both suffered from severely non-flat gain spectra, as do most FOPAs. In order to flatten the gain without the use of filters, researchers have recently investigated both multi-segment [4,13,14] and dual-pump designs [3,5,11,15,16].

In this paper, we revisit the simple single-pump, single-fiber optical parametric amplifier previously studied by several authors [1,7,17–20]. In particular, we further exploit the work of Marhic et al.,

* Corresponding author. Tel.: +558132718453; fax: +558132710359.
E-mail address: anderson@df.ufpe.br (A.S.L. Gomes).

0030-4018/$ - see front matter
doi:10.1016/S0030-4018(03)01624-9

where it was shown theoretically that gain spectra can be flattened and total bandwidth can be broadened by taking into account the fiber second- and fourth-order dispersion parameters β_2 and β_4 [1]. Here we concentrate our attention on the conditions required for obtaining a very flat, ripple-free gain band, thus ensuring gain uniformity over a large portion of the parametric gain spectrum. Design rules for achieving such broadband, flat parametric gain spectra are presented which are valid for any realistic set of fiber parameters, allowing the design of single-pump, single-fiber FOPAs with 3-dB bandwidths of over 40 nm (single-sided) and gain greater than 50 dB, which is ripple-free across ~30% of the total spectrum without the use of any gain flattening devices. The key to obtaining these results is the proper exploitation of the fiber second- and fourth-order dispersion parameters β_2 and β_4, respectively. After completion of this work, the article of [15] came to our attention, where some of their results agree entirely with some of the results found independently and reported here.

2. Theory

In the no-depletion approximation the parametric amplification is described by the signal power gain [1,18,21]

$$G_s(L) = \frac{P_s(L)}{P_s(0)} = 1 + \left[\frac{\gamma P_p}{g}\sinh(gL)\right]^2, \tag{1}$$

where P_p and P_s are the pump and signal powers in the fiber, γ is the fiber nonlinear coefficient ($\gamma = 2\pi n_2/\lambda A_{\text{eff}}$), L is the fiber length and g is the parametric gain parameter given by [1,21]

$$g^2 = (\gamma P_p)^2 - \kappa^2/4 = -\Delta\beta(\Delta\beta/4 + \gamma P_p), \tag{2}$$

where $\kappa = \Delta\beta + 2\gamma P_p$ and $\Delta\beta = \beta(\omega_s) + \beta(\omega_i) - 2\beta(\omega_p)$. Expanding the terms $\beta(\omega_s)$ and $\beta(\omega_i)$ around ω_p and retaining terms up to fourth-order yields

$$\Delta\beta = \beta_2\Omega^2 + \frac{\beta_4}{12}\Omega^4, \tag{3}$$

where $\Omega = \omega_s - \omega_p$ is the frequency detuning of the signal from the pump and $\beta_m = d^m\beta/d\omega^m|_{\omega=\omega_p}$. Note that the odd terms drop out of Eq. (3) since $\omega_i - \omega_p = -(\omega_s - \omega_p)$.

In order to have maximum parametric gain, the nonlinear phase mismatch κ should be equal to zero, i.e., the interaction should be phasematched. To illustrate this we show in Figs. 1(a) and (b) the behavior of the nonlinear phase mismatch and the corresponding fiber gain as a function of the signal detuning for a pump at 1550 nm. Note that we have shown only one side of the curves, which are approximately symmetric about the pump wavelength. To obtain these figures, we used $\gamma P_p = 15\ \text{km}^{-1}$, which could be easily achieved with a CW pump in a highly nonlinear fiber, $L = 0.20$ km, $\beta_4 = 2.5 \times 10^{-4}\ \text{ps}^4\ \text{km}^{-1}$, an experimental value found in the literature [1,21], and we varied β_2 from -0.030 to $-0.065\ \text{ps}^2/\text{km}$, typical values which one would obtain when pumping very near the zero-dispersion wavelength λ_0. For $\beta_2 = -0.030\ \text{ps}^2/\text{km}$ the interaction is never phasematched, however the gain spectrum has a maximum at the minimum of κ. On the other hand, when $\beta_2 = -0.065\ \text{ps}^2/\text{km}$, the interaction is phasematched for two different signal detunings, which leads to two peaks of maximum gain on each side of the gain spectrum. The depression in the gain spectrum between the two peaks is due to the non-zero phase mismatch in this region. Finally, when the minimum of κ coincides with $\kappa = 0$ (which occurs for $\beta_2 = -0.050\ \text{ps}^2/\text{km}$ in this example), we have a condition of minimum sensitivity to phase mismatch, and the corresponding gain spectrum exhibits a broadened, flattened band [15].

It is thus possible to find a relationship between β_2 and β_4, which results in a broadband, flat gain spectrum by requiring the minimum of κ (occurring at $\Omega^2 = -6\beta_2/\beta_4$) to coincide with the phasematch condition $\kappa = 0$. The resulting relationship, which is presented here for the first time in a simple form, is

$$\beta_2 = -\left(\frac{2}{3}\gamma P_p \beta_4\right)^{1/2}. \tag{4}$$

This relation shows the usual requirement of $\beta_2 < 0$ for broadband FOPAs, while also requiring β_4 to be positive [1]. The β_4 is assumed to be approximately constant over a large range of signal

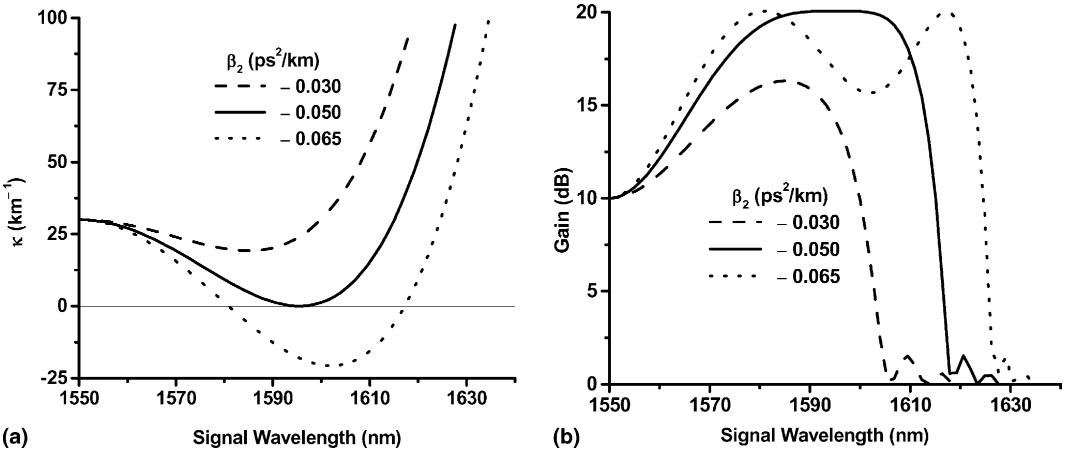

Fig. 1. Nonlinear phase mismatch (a) and gain spectra (b) obtained using $\beta_4 = 2.5 \times 10^{-4}$ ps^4 km^{-1}, with a fixed fiber nonlinearity $\gamma P_p = 15$ km^{-1} and a fiber length $L = 0.20$ km.

wavelengths near λ_0, while β_2 depends on the dispersion slope of the fiber and the detuning of the pump wavelength from λ_0. Given the dispersion values for wavelengths near λ_0, it is not difficult to determine the β_4 of the fiber [6,21]. Subsequently, Eq. (4) yields the β_2 and thus the pump wavelength required to achieve a flat gain spectrum for a given fiber.

3. Results of numerical simulations

In what follows, we demonstrate how the use of Eq. (4) results in flat, broadband gain spectra for any realistic set of experimental FOPA parameters. In all the figures which follow, we have constrained β_2 to the value given by Eq. (4) for the parameters used. While exhibiting behavior generally identical to gain calculations which neglect β_4, the important feature is that the spectra remain flat, indicating the generality of Eq. (4). Note that in Figs. 2–5 we show only the long-wavelength side of the total gain spectra for a pump wavelength of 1550 nm. In Fig. 2 we show several flat gain spectra which one obtains by varying β_4 from 1.0×10^{-4} ps^4 km^{-1} to 5.0×10^{-3} ps^4 km^{-1}, while fixing $\gamma P_p = 15$ km^{-1} and $L = 0.20$ km. We see that bandwidth increases significantly as β_4 is reduced, as expected since $|\beta_2|$ is simultaneously reduced, while spectral flatness is continually preserved over a large range of signal wavelengths.

In Fig. 3, we vary γP_p from 2 to 20 km^{-1}, while fixing the fiber length at $L = 0.20$ km and $\beta_4 = 2.5 \times 10^{-4}$ ps^4 km^{-1}. Again flatness is preserved, while the total gain bandwidth and the maximum gain increase as γP_p increases, as expected. The 3-dB bandwidth remains approximately constant (~40 nm) for γP_p values which leads to useful, i.e., >10 dB, gain spectra.

In Fig. 4 the fiber length is changed while maintaining $\beta_4 = 2.5 \times 10^{-4}$ ps^4 km^{-1} and $\gamma P_p = 15$ km^{-1}. We clearly see that the maximum flat

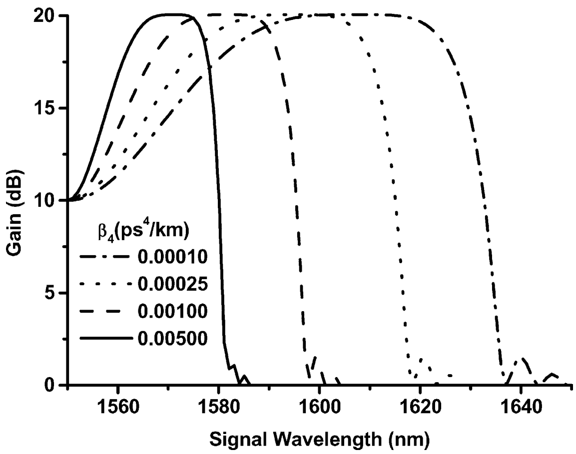

Fig. 2. Flat gain spectra obtained using values of β_2 given by Eq. (4) while varying β_4 from 1.0×10^{-4} ps^4 km^{-1} to 5.0×10^{-3} ps^4 km^{-1}, with a fixed fiber nonlinearity $\gamma P_p = 15$ km^{-1} and a fiber length $L = 0.20$ km.

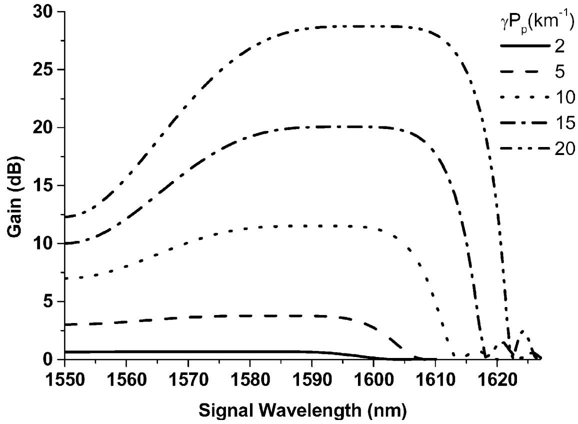

Fig. 3. Flat gain spectra obtained using values of β_2 given by Eq. (4) by varying γP_p, while fixing $\beta_4 = 2.5 \times 10^{-4}$ ps^4 km^{-1} and $L = 0.20$ km.

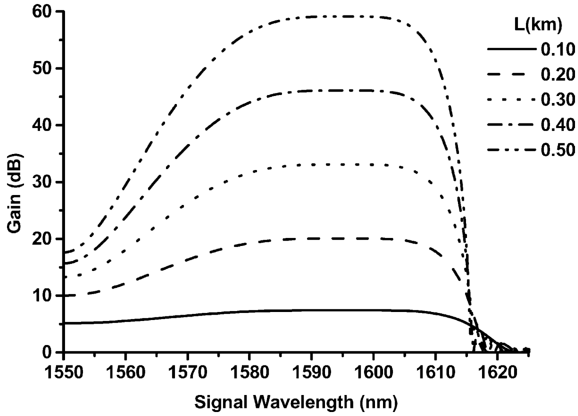

Fig. 4. Flat gain spectra obtained using values of β_2 given by Eq. (4) for various fiber lengths. Here $\beta_4 = 2.5 \times 10^{-4}$ ps^4 km^{-1} and $\gamma P_p = 15$ km^{-1}.

gain increases approximately linearly with L, as expected. The total gain bandwidth remains almost constant, whereas the 3-dB gain bandwidth diminishes slightly for long fiber lengths.

In Fig. 4 we see up to 60 dB gain for $L = 0.5$ km. Experimental values of $\sim$50 dB have already been demonstrated [2,7] and very recently, 60 dB gain has been experimentally demonstrated [22]. Note from Eq. (1) that the no-depletion approximation leads to unlimited growth of the gain as a function of the FOPA parameters, for example, the fiber length. Also, in this approximation the gain spectrum is independent of the input signal power. In practice, however, pump depletion and signal levels limit the maximum gain achievable [7,23], so these must be included if we want a realistic FOPA design.

Pump depletion is governed by the coupled equations, Eq. (5), that describe the evolution of the pump, signal, and idler along the fiber [7,17–19]

$$\begin{aligned} \frac{dP_p}{dz} &= -4\gamma\left(P_p^2P_sP_i\right)^{1/2}\sin\theta, \\ \frac{dP_s}{dz} &= 2\gamma\left(P_p^2P_sP_i\right)^{1/2}\sin\theta, \\ \frac{dP_i}{dz} &= 2\gamma\left(P_p^2P_sP_i\right)^{1/2}\sin\theta, \\ \frac{d\theta}{dz} &= \Delta\beta + \gamma\left\{2P_p - P_s - P_i + \left[\left(P_p^2P_i/P_s\right)^{1/2} \right.\right. \\ &\quad \left.\left. + \left(P_p^2P_s/P_i\right)^{1/2} - 4(P_sP_i)^{1/2}\right]\cos\theta\right\}, \end{aligned} \tag{5}$$

P_p, P_s, and P_i are the pump, signal and idler powers in the fiber and θ is a relative phase factor between the fields, defined as $\theta(z) = \Delta\beta z + \phi_s(z) + \phi_i(z) - 2\phi_p(z)$, where ϕ_s, ϕ_i and ϕ_p are the phases of the respective fields. The set of Eqs. (5) can be analytically solved for the case where fiber loss is neglected [19,24,25] as briefly explained in Appendix A.

In Fig. 5 we show the evolution of the gain spectrum obtained using these equations as the

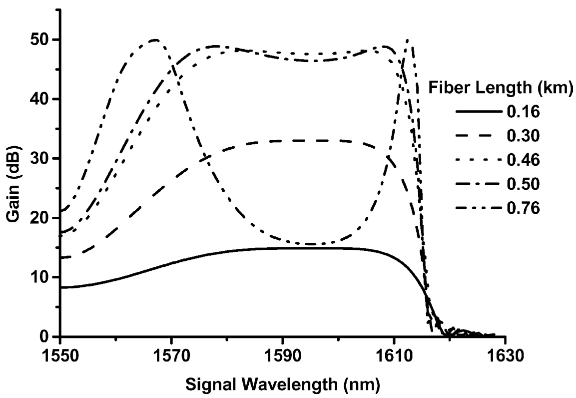

Fig. 5. Gain spectra calculated using analytical solutions of the coupled mode equations while varying the fiber length. Maximum depletion of the pump (at the central frequency) occurs for $L \approx 0.46$ km. Here, $\beta_2 = -0.050$ ps^2/km, $\beta_4 = 2.5 \times 10^{-4}$ ps^4/km, $\gamma = 15$ W^{-1} km^{-1}, $P_{p0} = 1$ W and $P_{s0} = 5$ μW.

fiber length increases while keeping β_2 and β_4 linked by Eq. (4). The depression in the gain occurring for longer fiber lengths results from back conversion related to the nonlinear phase mismatch in the strong depletion regime, which not only depends on pump power but also on signal and idler powers and distance along the fiber z, and is given by $\kappa(z) = \Delta\beta + \gamma(2P_p(z) - P_s(z) - P_i(z))$ [7,19]. In Fig. 5 there is clearly a limit to the maximum gain that can be obtained at the central wavelength corresponding to the detuning $\Omega^2 = -6\beta_2/\beta_4$ which is related to the maximum pump depletion possible. In fact, as can be seen in Eq. (5), pump is converted in signal and idler power while θ is positive. If θ is negative, signal and idler are converted back to pump power. It can be shown [19], that the pump power oscillates periodically along the fiber. An approximate expression for the fiber length that gives the maximum pump depletion is obtained in Appendix A:

$$L_{opt} \approx \frac{1}{2\gamma P_0} \ln \frac{16P_0}{3P_{s0}}. \quad (6)$$

Here, P_0 is the total power which can also be written as $P_0 = P_{p0} + P_{s0}$, where P_{p0} and P_{s0} are the input pump and signal powers in the fiber, respectively. For the conditions of Fig. 5, this results in $L_{opt} = 0.46$ km. However, when using this optimum fiber length and the condition of flat gain obtained in the no-depletion approximation, Eq. (4), there appears a slight ripple in the spectrum for L_{opt}, as can be seen in Fig. 5. This happens because the nonlinear phase mismatch κ, used to derive Eq. (4), is no longer given by $\kappa = \Delta\beta + 2\gamma P_{P0}$ as this is valid only in the no-depletion approximation. Clearly, the condition of flatness given by (4) is no longer valid and has to be modified. We have observed, after several simulations, that the ripple occurring using (4) and (6) depends on P_{s0}/P_{p0}. In this way we were able to obtain an empirical correction for condition (4) which is found to be

$$\beta_2 = -\sqrt{\frac{2}{3}\gamma P_{p0}\beta_4}\left[1 - 0.33\left(\frac{P_{s0}}{P_{p0}}\right)^{1/6}\right]. \quad (7)$$

As also shown in Appendix A, the maximum flat gain obtained using Eqs. (6) and (7) is, to a good approximation, given by

$$G_{max}^{flat}\ (\mathrm{dB}) \approx 10\log\left(\frac{2P_0}{7P_{s0}}\right). \quad (8)$$

The result is, however, always slightly less than the result of the analytic solution. More explicitly, for high values of the ratio P_{s0}/P_0 such as 0.1, the maximum gain obtained by Eq. (8) is below the exact value calculated using Eqs. (6) and (7) and the analytic solution by 1.5 dB, but for lower, more realistic ratios, say 10^{-4}–10^{-6}, the value given by Eq. (8) is only 0.5 dB below the exact value, which is a small error since the gains for this power ratio are above 30 dB.

The optimum length and the resulting maximum flat gain are key parameters of flat FOPAs. Eqs. (6) and (8) relate these design parameters with the input pump and signal powers in the fiber and the fiber nonlinear coefficient γ. We can also see in Fig. 5 that a trade-off exists between spectral flatness and gain bandwidth. Increasing the fiber length slightly beyond the optimum value for flatness, i.e., to $L = 0.50$ km here, results in a significantly larger 3-dB bandwidth with a minimal increase in gain ripple, which may be an acceptable trade-off in a given system.

4. Conclusions

In this paper, we have demonstrated that the proper exploitation of the dispersion parameters β_2 and β_4 can result in ripple-free, broadband parametric gain spectra with 50 dB or more of gain and more than 40 nm of single-sided bandwidth. We have developed design rules for obtaining such gain spectra which are valid for any combination of realistic experimental parameters, supported by numerical simulations and analytical analysis. Important avenues for future work are the experimental demonstration of the predicted flat gain spectra, and the inclusion in the model of conditions to be found in a real DWDM system. Such conditions are the finite bandwidth of the pump, the effects of several simultaneous signal channels, sensitivity to polarization mode dispersion (PMD) and the degradation of amplifier performance due to random variations of parameter values along the length of the fiber [26].

Acknowledgements

This work was supported by the Research and Development Center, Ericsson Telecomunicações S. A., Brazil. C. Floridia acknowledges scholarship support from the Brazilian agency CNPq. The authors thank the referees for valuable suggestions.

Appendix A

In this section we explain the steps used to obtain Eq. (6). The coupled set of Eq. (5) can be solved analytically [19,24,25]. To accomplish this we first recognize the invariants [19]:

$$P_0 = P_{\mathrm{p}}(z) + P_{\mathrm{s}}(z) + P_{\mathrm{i}}(z) = P_{\mathrm{p}0} + P_{\mathrm{s}0}, \tag{A.1}$$

$$\alpha = \frac{P_{\mathrm{s}}(z) - P_{\mathrm{i}}(z)}{P_0} = \frac{P_{\mathrm{s}0}}{P_0}, \tag{A.2}$$

$$H = \frac{1}{P_0^2}\left(4P_P(z)\sqrt{P_{\mathrm{s}}(z)P_{\mathrm{i}}(z)}\cos\theta(z) - \left(\frac{\Delta\beta}{\gamma P_0} - 1\right)P_{\mathrm{p}}(z)P_0 - \frac{3}{2}P_{\mathrm{p}}^2(z)\right), \tag{A.3}$$

where P_0 is the total power in the fiber. Also the initial idler power is $P_{\mathrm{i}}(0) = P_{\mathrm{i}0} = 0$.

Using these invariants in the first of the coupled equations (5) we obtain

$$\frac{\mathrm{d}\eta}{\mathrm{d}\xi} = \pm\sqrt{f(\eta)}, \tag{A.4}$$

where $\eta = P_{\mathrm{p}}(z)/P_0$ and $\xi = \gamma P_0 z$ are the normalized pump power and the normalized distance and

$$f(\eta) = 4\eta^2[(1-\eta^2) - \alpha^2] - \left[H + \left(\frac{\Delta\beta}{\gamma P_0} - 1\right)\eta + \frac{3}{2}\eta^2\right] \tag{A.5}$$

is a polynomial of fourth-order in η. It can be shown that Eq. (A.4) can be integrated so that the normalized pump power along the fiber is given by [24]

$$\eta(\xi) = \frac{\eta_2 - \eta_0\eta_1 sn^2\left(\frac{\xi - z_0}{z_c}|k\right)}{1 - sn^2\left(\frac{\xi - z_0}{z_c}|k\right)}, \tag{A.6}$$

where η_1, η_2, η_3 and η_4 are the roots of the fourth-order polynomial (A.5) in ascending order. The function $sn(u|m)$ is the Jacobian elliptic function [27] and

$$\eta_0 = \frac{\eta_3 - \eta_2}{\eta_3 - \eta_1}, \tag{A.7}$$

$$k^2 = \frac{\eta_3 - \eta_2}{\eta_3 - \eta_1}\frac{\eta_4 - \eta_1}{\eta_4 - \eta_2}, \tag{A.8}$$

$$z_c = \frac{2}{\left(\frac{7}{4}(\eta_3 - \eta_1)(\eta_4 - \eta_2)\right)^{1/2}}, \tag{A.9}$$

$$z_0 = z_c F\left(\sin^{-1}\left(\sqrt{\frac{P_{\mathrm{p}0} - P_0\eta_2}{\eta(P_{\mathrm{p}0} - P_0\eta_1)}}\right), k\right) \tag{A.10}$$

where $F(u,m)$ is the elliptic integral of first kind associated with the complete elliptic integral $K(m)$ [27].

The function $sn(u|m)$ is periodic with period of $4K(m)$ so that the normalized pump power has a spatial period $\xi_{\mathrm{p}} = z_{\mathrm{c}}2K(k)$. Therefore the normalized pump experiences maximum depletion for half of this period, which occurs when the phase $\theta = 0$ as discussed before. This defines our optimum fiber length

$$z_{\mathrm{opt}} = \frac{z_{\mathrm{c}}}{\gamma P_0}K(k). \tag{A.11}$$

Eq. (A.11) can be further simplified if we evaluate the invariants (at $z = 0$) for the central frequency, defined to be the frequency where the minimum of κ occurs. As we have already shown this frequency corresponds to a detuning $\Omega^2 = -6\beta_2/\beta_4$. Setting $\kappa_{\min} = 0$ at this frequency (flat spectrum condition), we have $\Delta\beta = -2\gamma P_{\mathrm{p}0}$ so that:

$$\frac{\Delta\beta}{\gamma P_0} \approx \frac{\Delta\beta}{\gamma P_{\mathrm{p}0}} = -2, \tag{A.12}$$

$$H \approx \frac{3}{2}, \tag{A.13}$$

$$\alpha = \frac{P_{\mathrm{s}0}}{P_0}. \tag{A.14}$$

We note here that the use of the flat spectrum condition in the no-depletion regime is valid since we are evaluating the invariant at the fiber input where depletion certainly does not occur.

Using Eqs. (A.12)–(A.14) we can find the roots of Eq. (A.5) for the central frequency. The roots will depend only on α. The quantities z_c and k^2 can then be expanded in terms of α (since generally $\alpha \ll 1$, or in other words the input signal power is very small compared with the total power). The Taylor expansions of these quantities read:

$$z_c \approx 1, \tag{A.15}$$

$$k^2 \approx 1 - 3\alpha. \tag{A.16}$$

Now we use the asymptotic form of $K(k)$ for k approaching unity [27]

$$K(k) \approx \frac{1}{2}\ln\frac{16}{1-k^2} \approx \frac{1}{2}\ln\frac{16}{3\alpha}. \tag{A.17}$$

In this way L_{opt} is given by

$$L_{opt} = z_{opt} \approx \frac{1}{2\gamma P_0}\ln\frac{16P_0}{3P_{s0}}. \tag{A.18}$$

It is now possible to evaluate the pump power at the length L_{opt}. Since at L_{opt} the $sn^2(u|m)$ of Eq. (A.6) is zero, we have

$$P_p(L_{opt}) = P_0\eta_2 \approx \frac{3}{7}P_0, \tag{A.19}$$

where η_2 expanded in a Taylor series reads $\eta_2 \approx (3/7) + (3/8)\alpha^2$.

In this way, the signal power along the fiber, which is given by

$$P_s(z) = \frac{P_0(1+\alpha) - P_p(z)}{2}, \tag{A.20}$$

becomes at L_{opt}

$$P_s(L_{opt}) \approx \frac{P_0(1+\alpha) - (3/7)P_0}{2} = \frac{P_0}{2}\left(\frac{4}{7}+\alpha\right). \tag{A.21}$$

It follows that an estimate of the maximum gain at the central frequency (at L_{opt}) is given by

$$G_{max} = 10\log\left(\frac{P_s(L_{opt})}{P_{s0}}\right) \approx 10\log\left(\frac{2}{7\alpha}+\frac{1}{2}\right) \approx 10\log\left(\frac{2P_0}{7P_{s0}}\right). \tag{A.22}$$

References

[1] M.E. Marhic, N. Kagi, T.-K. Chiang, L.G. Kazovsky, Opt. Lett. 21 (1996) 573.

[2] J. Hansryd, P.A. Andrekson, IEEE Photon. Technol. Lett. 13 (2001) 194.

[3] M.E. Marhic, Y. Park, F.S. Yang, L.G. Kazovsky, Opt. Lett. 21 (1996) 1354.

[4] L. Provino, A. Mussot, E. Lantz, T. Sylvestre, H. Maillotte, in: Technical Digest of the Optical Fiber Communication Conference, Optical Society of America, Washington, DC, 2002, p. 125.

[5] K.K.Y. Wong, M.E. Marhic, K. Uesaka, L.G. Kazovsky, in: Technical Digest of the Optical Fiber Communication Conference, Optical Society of America, Washington, DC, 2002, p. 129.

[6] M.C. Ho, K. Uesaka, M.E. Marhic, Y. Akasaka, L.G. Kazovsky, IEEE J. Lightwave Technol. 19 (2001) 977.

[7] K. Inoue, T. Mukai, Opt. Lett. 26 (2001) 10.

[8] J.L. Blows, S.E. French, Opt. Lett. 27 (2002) 491.

[9] C.J.S. de Matos, D.A. Chestnut, P.C. Reeves-Hall, J.R. Taylor, Opt. Lett. 26 (2001) 1583.

[10] D.A. Chestnut, C.J.S. de Matos, J.R. Taylor, J. Opt. Soc. Am. B 19 (2002) 1901.

[11] J.M. Chávez Boggio, F.A. Callegari, S. Tenenbaum, H.L. Fragnito, J.B. Rosolem, M.R.X. de Barros, in: Technical Digest of the Optical Fiber Communication Conference, Optical Society of America, Washington, DC, 2002, p. 636.

[12] J. Hansryd, P. Andrekson, M. Westlund, J. Li, P.-O. Hedekvist, IEEE J. Sel. Top. Quantum Electron. 8 (2002) 506.

[13] S.E. French, J.L. Blows, in: N. Jolley, J.D. Minelly, Y. Nakano (Eds.), Optical Amplifiers and their Applications, OSA Trends in Optics, Photonics Series, vol. 60, Optical Society of America, Washington, DC, 2001, p. 88.

[14] M.E. Marhic, M.C. Ho, L.G. Kazovsky, IEEE J. Lightwave Technol. LT-17 (1999) 210.

[15] C.J. McKinstrie, S. Radic, A.R. Chraplyvy, IEEE Sel. Top. Quantum Electron. 8 (2002) 538.

[16] J.M. Chávez Boggio, S. Tenenbaum, H.L. Fragnito, J. Opt. Soc. Am. B 18 (2001) 1428.

[17] A. Vatarescu, IEEE J. Lightwave Technol. LT-5 (1987) 1652.

[18] R.H. Stolen, J.E. Bjorkholm, IEEE J. Quantum Electron. QE-18 (1991) 824.

[19] G. Cappellini, S. Trillo, J. Opt. Soc. Am. B 8 (1991) 824.

[20] M. Yu, C.J. McKinstrie, Phys. Rev. E 52 (1995) 1072.

[21] G.P. Agrawal, Nonlinear Fiber Optics, second ed., Academic Press, San Diego, CA, 1995.

[22] M.E. Marhic, in: Technical Digest of the Optical Fiber Communication Conference, Optical Society of America, Washington, DC, 2003, p. 564.

[23] M.E. Marhic, K.K.Y. Wong, M.C. Ho, L.G. Kazovsky, Opt. Lett. 26 (2001) 620.

[24] Y. Chen, J. Opt. Soc. Am. B 6 (1989) 1986.
[25] Y. Chen, A.W. Snyder, Opt. Lett. 14 (1989) 87.
[26] M. Karlsson, J. Opt. Soc. Am. B 15 (1998) 2269.
[27] I.S. Gradshteyn, I.M. Ryzhik, Table of Integrals, Series, and Products, Corrected and Enlarged Edition, Academic Press, San Diego, CA, 1980.